PAPER

First dust study in JET with the ITER-like wall: sampling, analysis and classification

To cite this article: A. Baron-Wiechec *et al* 2015 *Nucl. Fusion* **55** 113033

IOP Publishing | International Atomic Energy Agency Nuclear Fusion

Nucl. Fusion **55** (2015) 113033 (7pp) doi:10.1088/0029-5515/55/11/113033

First dust study in JET with the ITER-like wall: sampling, analysis and classification

A. Baron-Wiechec[1], E. Fortuna-Zaleśna[2], J. Grzonka[2], M. Rubel[3], A. Widdowson[1], C. Ayres[1], J. P. Coad[1], C. Hardie[1], K. Heinola[4], G. F. Matthews[1] and JET Contributors[5]

EUROfusion Consortium, JET, Culham Science Centre, Abingdon, OX14 3DB, UK
[1] CCFE, Culham Science Centre, Abingdon, OX14 3DB, UK
[2] Faculty of Materials Science and Engineering, Warsaw University of Technology, 02-507 Warsaw, Poland
[3] Department of Fusion Plasma Physics, Royal Institute of Technology (KTH), 100 44 Stockholm, Sweden
[4] University of Helsinki, PO Box 64, 00014 University of Helsinki, Finland

E-mail: Aleksandra.Baron-Wiechec@ccfe.ac.uk

Received 14 July 2015, revised 7 September 2015
Accepted for publication 18 September 2015
Published 15 October 2015

Abstract

Results of the first dust survey in JET with the ITER-Like Wall (JET-ILW) are presented. The sampling was performed using adhesive stickers from the divertor tiles where the greatest material deposition was detected after the first JET-ILW campaign in 2011–2012. The emphasis was especially on sampling and analysis of metal particles (Be and W) with the aim to determine the composition, size, surface topography and internal dust structure using a large set of methods: high-resolution scanning and transmission electron microscopy, focused ion beam, electron diffraction and also wavelength and energy dispersive x-ray spectroscopy. The most important was the identification of beryllium dust both in the form of flakes and droplets with dimensions in the micrometer range. Tungsten, molybdenum, inconel constituents were identified along with many impurity species. The particles are categorised and the origin of the various constituents discussed.

Keywords: dust, JET, ITER-like wall, beryllium, tungsten erosion-deposition

(Some figures may appear in colour only in the online journal)

1. Introduction

Concerns regarding reactor safety and diagnostic performance in a reactor-class device (e.g. ITER) are the main driving force for dust studies in current devices. Their aim is to build a prudent database for the prediction of major formation mechanisms and to assess the amount and form of dust. It is crucial for the licensing process especially in connection with operation using a deuterium-tritium fuel mixture. Very thorough dust surveys have been carried out regularly at several tokamaks: TEXTOR [1–9], ASDEX-Upgrade [10–13], JET [14–16], Tore Supra [17], DIII-D [18], KSTAR [19] and other machines, as summarised by Braams [20]. JET is the most relevant machine from the reactor point of view, because of the full metal wall composed of beryllium in the main chamber and tungsten in the divertor: the ITER-Like Wall (JET-ILW) in operation since August 2011 [21–24]. As a consequence, the major challenge in dealing with the in-vessel materials from the JET-ILW is the contamination by beryllium and tritium originating both from a residue remaining after the earlier D-T operation [25] and from the D-D reactions.

This paper is focused in particular on the comprehensive characterisation of metal particles: their composition, structure including internal features of droplets and splashes. In the following paragraphs the dust sampling and relevant analytical approach and apparatus are introduced. The dust and debris identified are categorised firstly into particles originating from the major wall constituents: beryllium, tungsten and tungsten-molybdenum and secondly in to particles mixed materials containing carbon, ceramic components and other species.

[5] See appendix of [40].

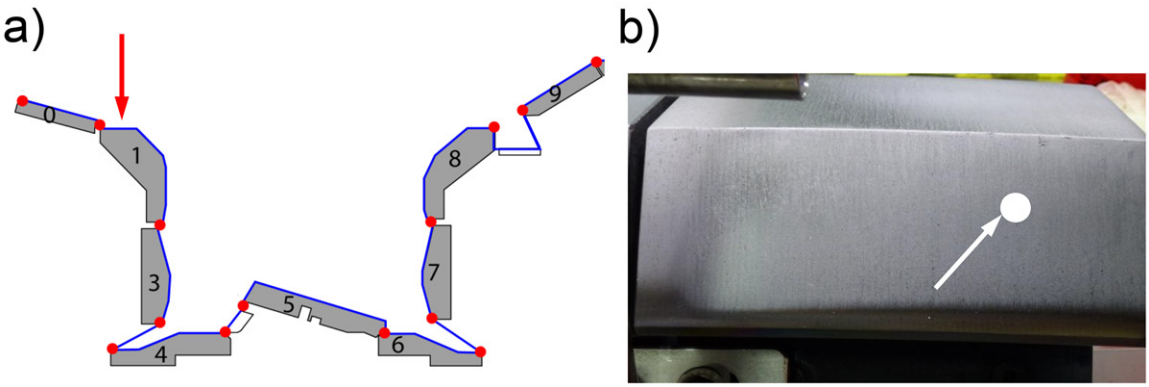

Figure 1. (a) Divertor cross-section in JET-ILW with marked position of the apron on Tile 1 in the inner divertor (b) and image of Tile 1 with the dust sampling position.

2. Experimental

2.1. Dust sampling

Two types of dust collection were performed after venting JET-ILW during its first shut-down. Firstly, *in situ* dust removal by vacuum cleaning of tiles in 22 (out of 24) divertor modules was done using a special nozzle installed on a remotely handled robotic arm. Secondly dust from the outer divertor and its inner leg was retrieved to separate containers. The mass of loose matter removed from the tiles was slightly below 1 gram, as reported in [16]. This amount was very small in comparison to that removed by the same means after the last operation period with carbon walls, i.e. in JET-C: nearly 200 g [26].

Another sampling operation was done manually when two not vacuum cleaned divertor modules were transferred from the torus to the Beryllium Handling Facility (BeHF) for the exchange of erosion-deposition probes installed on those modules [27]. The visual inspection allowed for the identification of a zone with the greatest deposition (confirmed in [26, 28–31]) located on the so-called apron of Tile 1 in the inner divertor. The tiles in the inner (0;1;3;4) and the outer (6;7;8;9) divertor are made of carbon fibre composite (CFC) with surfaces coated by tungsten (14–20 μm) with a 3–4 μm interlayer of molybdenum between CFC and W.

The divertor cross-section and the apron position are shown in figure 1(a), while an image in figure 1(b) shows the tile surface with the marked area of dust sampling using standard carbon sticky pads of 2.54 cm (1 inch) in diameter. The advantages of manual sampling are: (i) a direct correlation between the location and the type of dust particles; (ii) small amounts of contaminated material are firmly bound to the substrate thus eliminating possibility of flaking in the surface analysis station. There is also an obvious disadvantage arising from the fact that only the bottom side of the collected matter can be examined by standard microscopy methods, i.e. surface facing substrate of the tile but not the plasma-facing side. Fortunately, this may be partly overcome by cross-sectional analysis using focused ion beam (FIB), as addressed in section 3. Only two specimens were taken to test whether such materials could later be accepted for laboratory studies knowing that the examination would require high-resolution equipment with beryllium detection capabilities.

2.2. Analysis methods

The study was performed using a broad range of electron and ion methods at the Warsaw University of Technology (WUT) and at the Culham Centre for Fusion Energy (CCFE). The analyses performed at WUT comprised high-resolution scanning electron (SEM) and transmission (STEM) microscopy, FIB, electron diffraction and wavelength and energy dispersive x-ray spectroscopy, WDS (MAXray PBS -Parallel Beam Spectrometer -Thermo NORAN) and EDS, respectively. Scanning microscopy (Hitachi SU-70 FE-SEM, beam energy 0.3–30 keV, Hitachi SU8000, beam energy 0.5–30 keV) was combined with energy-dispersive x-ray spectroscopy (EDS Thermo Scientific Ultra Dry, type SDD—silicon drift detector) and YAG BSE (backscattered electron) detector. The internal morphology of selected particles was determined by means of focused ion beam (FIB/SEM Hitachi NB5000) and then STEM (Aberration Corrected Dedicated STEM Hitachi HD-2700, energy 80–200 keV) techniques. In FIB sampling for TEM a Ga^+ ion beam at 40 keV was used. Heavier species than Be were analysed also by SEM and EDS at CCFE using a TESCAN Mira3 XMH FE-SEM microscope (10–30 keV) equipped with an X-Max 80 EDS detector from Oxford Instruments.

To ensure proper identification of beryllium with WDS and EDS-SDD type tests were performed on a pure beryllium reference. A clear Be feature was obtained with WDS. In the case of EDS-SDD the spectrum, apart from the Be K_α line (108 eV), also contained traces of carbon and oxygen. The likely source of oxygen to the reference target occurred when transferring the sample from the vacuum sealed package to the microscopy chamber via atmosphere leading to surface oxidation. However some contamination by oxygen in the sample manufacturing process cannot be fully excluded. The presence of carbon is mainly due to the electron beam-induced deposition of carbon-containing species in the microscope chamber. Attenuation of the Be signal by a thin carbon film deposited on Be was also studied.

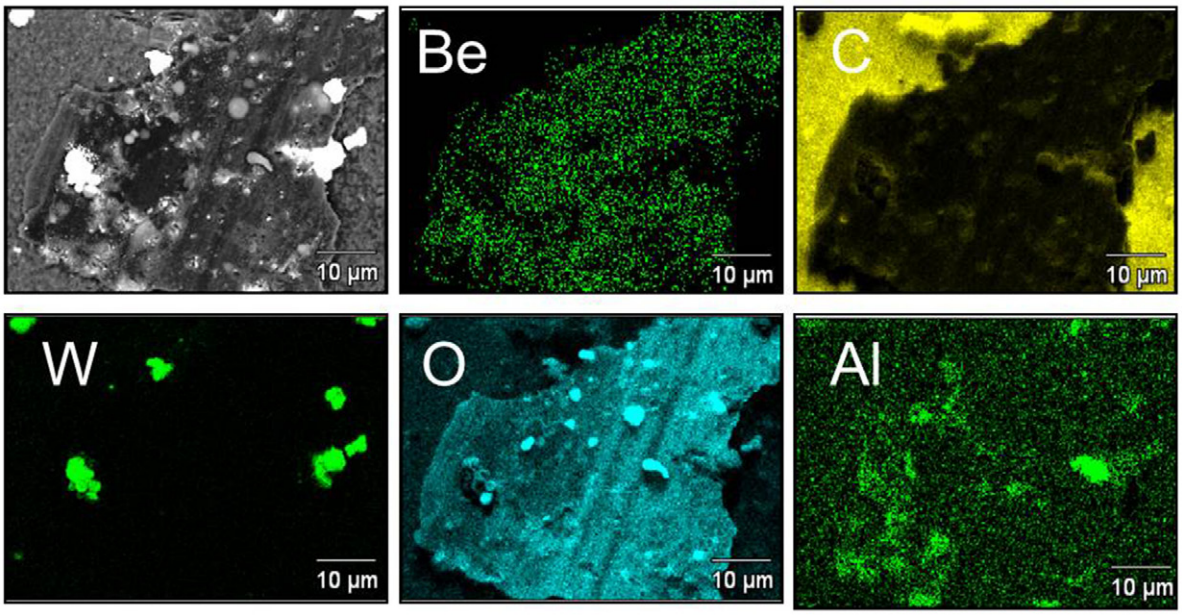

Figure 2. Beryllium flake detached from the deposit and the distribution of respective elements in the studied area.

The distribution and content of fuel in the respective dust grains was not studied for technical reasons. It has been known from the nuclear reaction analyses with a He-3 beam [28–32] that deposits on Tile 1 contain deuterium and beryllium. An attempt to use ion beam methods has been performed but the lateral resolution, even in the micro-beam version, is lower than that required for very detailed mapping of objects with dimensions in the low micrometer range.

3. Results and discussion

3.1. Beryllium

Two major types of beryllium-rich particles have been identified: (i) flakes of co-deposits and (ii) small spheres related to melting events of the Be limiters. A micrograph in figure 2 shows a flake, while the x-ray mapping in the associated frames gives a detailed overview of elemental composition and the distribution of Be, C, W, O and Al; the latter element most probably from the ceramic diagnostic or heating systems in JET. To our knowledge, it is the first result on the EDS identification of Be in co-deposits formed in a tokamak. One perceives that Be is the major component of the flake. The presence of oxygen over the entire flake area is most probably related to the surface oxidation when the tile retrieved from JET was exposed to air. This statement is supported by FIB/TEM studies described in the next paragraph. Only traces of carbon are detected on the flake, while the carbon signal in the flake-surrounding area is related to the glue on the sticker. The presence of small tungsten particles suggests that the flake was detached from the tile surface together with some micrometer size pieces of the W coating and also small W droplets; the latter is exemplified in figure 3(a). Other elements identified in trace quantities on the flake were sodium, chlorine, sulphur and phosphorus. The flake size is approximately 50×70 μm. Several such objects of a very similar size have been found on the sticker. It should be stressed that only very few small pieces of the Be-rich deposit were attached to sticker thus indicating that the deposited Be layer adheres firmly to the underlying substrate. As a result, no flaking co-deposits from the tungsten tile coating have been observed.

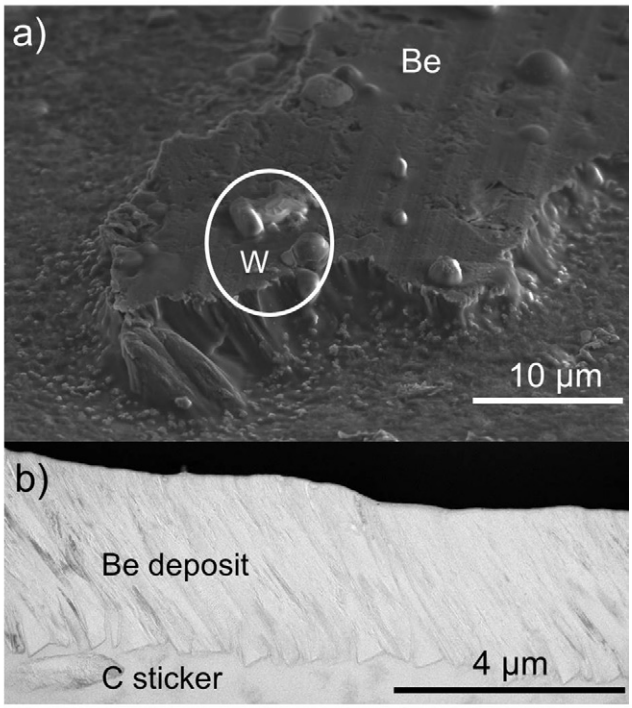

Figure 3. Beryllium flake (a) and its cross-section revealing the crystalline nature of the deposit (b).

Images in figures 3(a) and (b) show a detailed structure of the flake and its internal structure revealed by FIB. These are the first images showing fine features of the Be co-deposit. The layer has columnar structure and electron diffraction by TEM

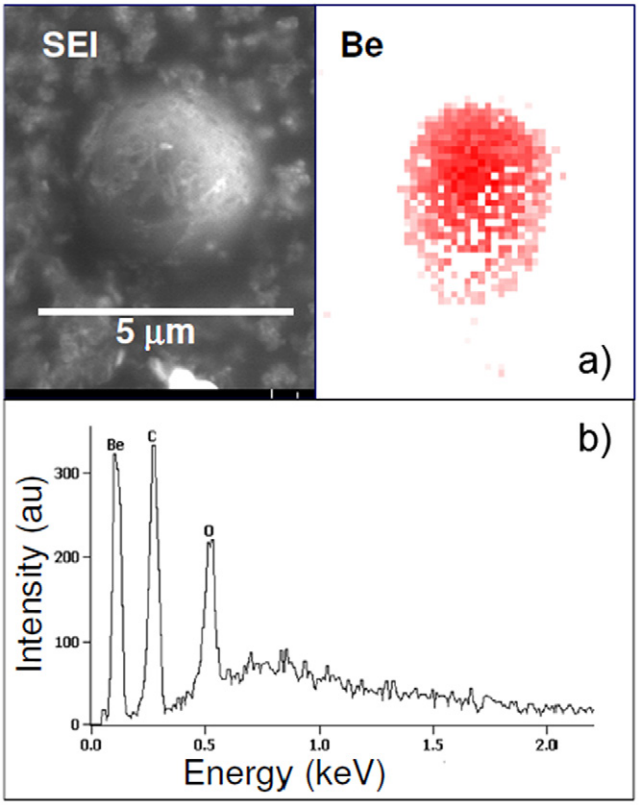

Figure 4. Beryllium droplet and distribution of beryllium on the surface (a) and the respective x-ray spectrum obtained by EDS (b).

proves its crystalline character. It suggests a steady growth of the layer during the JET operation. Oxygen is only a minor constituent of the layer thus indicating that the object of study is mainly beryllium, not its oxide. The thickness assessed from the micrographs, 4–7 μm, is in reasonable agreement with cross-sectional and ion beam analyses of co-deposits on the apron of Tile 1 [28, 29, 31, 32].

In figure 4 a secondary electron image (SE) of a small Be droplet (below 5 μm in diameter) is presented. The related mapping and the energy dispersive x-ray spectrum reveals beryllium as the major constituent: 70% Be, 20% C and 10% O, all in atomic per cent. Several objects of that type and size have been found. The formation of droplets originating from the melt layer splashing from the Be limiters had been expected, but their presence has not be documented earlier. However, from the image of particles embedded in the glue of the sticker it is difficult to conclude whether these are regular spheres of the original shape or droplets flattened on collision with the tile surface. Comet-like elongated splashes, such as described in our earlier work on metal dust [9] have not been detected.

3.2. Tungsten and molybdenum

Two distinct types of particles containing mainly high-Z metals have been detected: (i) agglomerates containing either only of those metals (W or W-Mo) or with addition of carbon and—in several cases—other species such as nickel, aluminium, silicon, boron nitride and oxygen; (ii) small spherical ball-like objects.

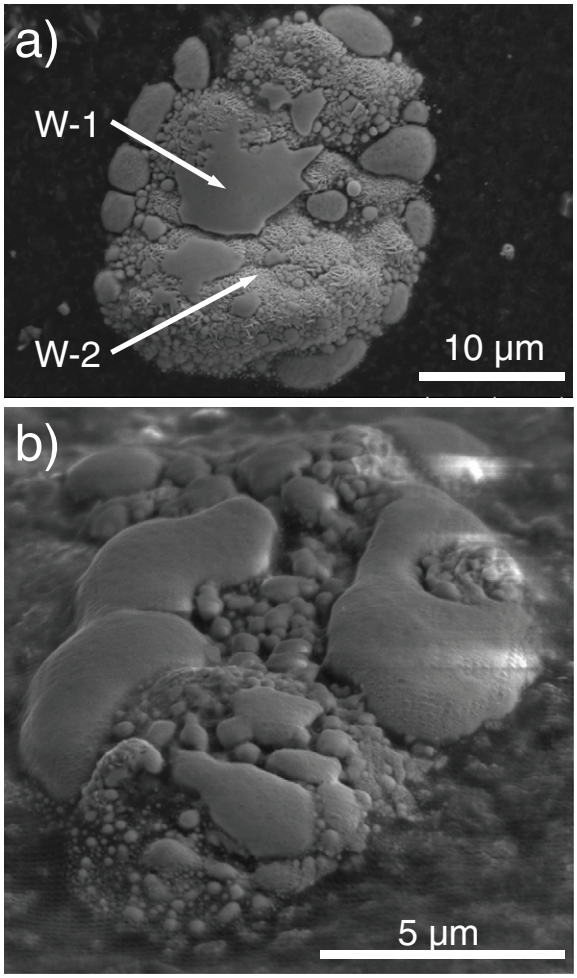

Figure 5. Tungsten-containing agglomerates originating from W coatings: W-Mo particle with marked areas of molten W-1 and original W-2 coating (a) and a mixed W-Mo-C particle (b).

Images in figure 5 show particles of the agglomerate type. The object in figure 5(a) is composed only of tungsten though the image reveals two different structures. Most probably it is a small piece of the W coating which was detached from the substrate and was partly molten. In the image the molten part is marked as W-1, while the part resembling the original layer is marked W-2. Figure 5(b) shows surface topography of the agglomerate, 8 $\times$ 15 μm in size, composed of a large number of molten fragments from 0.2 μm to 5 μm in linear dimension. The inner structure and composition of that object is documented in figures 6(a)–(c). Two phases of tungsten are found. Electron diffraction has proven the molten W-1 phase to be amorphous thus giving a strong indication on fast cooling of tungsten, which may lead to the formation of glassy metals [33]. A crystalline phase, W-2, is clearly seen inside the agglomerate. In addition to tungsten the crystalline part contains a molybdenum layer separating W from carbon, most probably CFC, as can be inferred from the structural details of the title. The presence of the shell with amorphous droplets 'shielding' the crystalline part may suggest that the agglomerate of that morphology was not formed locally on the apron of Tile 1. It is rather a flake from the W coating detached/eroded from the tungsten-coated tiles in the main

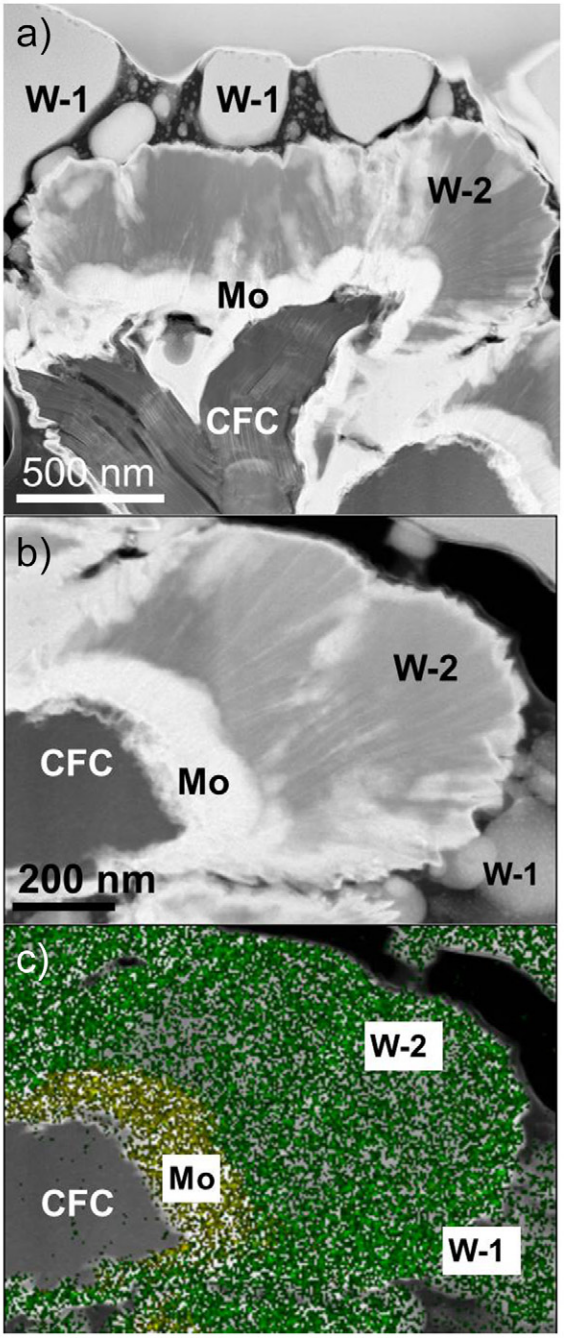

Figure 6. Internal structure and composition of the particle shown in figure 5(b): amorphous W-1 and crystalline W-2 phases and distribution of W, Mo and carbon fibre.

chamber, e.g. in the shine-through region of neutral beams. This is to some extent speculation, but justified as the strike point has never been positioned on the apron. It is also rather improbable that the area was overheated in disruptions. This statement is supported by earlier SEM observations which did not detect surface melting or recrystallization of the coating in that region [34]. A thickness of the Mo interlayer (around 120–150 nm) is much smaller than on plasma-facing surfaces of the coated W/Mo-CFC tiles: 3–4 μm of Mo. It suggests that the piece may originate from side surface of a tile, where coatings are of not-uniform thickness.

Recrystallized grains are clearly seen in the case of two rounded objects, 5μm in diameter, composed of tungsten which are shown in figures 7(a) and (b). The first image may suggest a solid metal splash (many particles of that type were found), but the other reveals a broken shell and an empty interior. This may suggest that the object is a cluster of smaller W molten grains which gradually pieced together. Such small structures have been observed earlier on the tungsten coating in TEXTOR [35]. A particle shown in figure 7(c) was sectioned by the Ga^+ beam to reveal the particle's shape and internal structure. It is a regular empty sphere with a uniform crystalline skin, 0.5 μm thick. Similar forms were detected earlier at ASDEX-Upgrade [12], which also uses W coatings on carbon plasma-facing components (PFC). Some options regarding the nucleation and growth processes of such objects were proposed. The authors suggest that the most reasonable option is the attachment of material towards clustering when small fragments are transported in the scrape-off layer (SOL) [12]. One may also suggest another possible mechanism: a tiny flake detached from the coating (80–120 μm^2) is a precursor. It enters plasma and by ablation in the rotational motion forms a regular rounded structure. A spherical shape of particles (both carbon and metals) has been documented earlier [3, 9, 12] and, also the evidence of rotational motion of hot dust particles in magnetic field has been shown and discussed [7, 9]. The origin of the empty interior could be associated with the occlusion of gas, i.e. deuterium, whose pressure makes the object spherical. In this sense, spheroids could be considered as bubbles.

3.3. Carbon and ceramic particles

A large number of particles having different constituents, shape and size have been detected. They belong to three groups: carbon, ceramics and metals namely steel or Inconel alloy components. Carbon, as discussed in section 3.2, may occur together with high-Z metals, when coatings are eroded. Pure carbon objects have also been detected. In the case of ceramics a list of frequently found elements comprises aluminium, silicon, barium, some sodium and magnesium which most probably originate from ceramics in heating or diagnostic systems. Another category is boron nitride: a material of the reciprocating probe heads. An entry of the probe to the plasma edge is accompanied by a release of a large plume of material, as shown in figure 8. A significant amount of small debris with stoichiometric boron nitride have been found thus indicating that the effect shown in figure 8 is not only the outgassing of the probe material but also macroscopic damage. This statement is supported by earlier studies when the deposition of BN dust was observed on the electrical and collector probe heads [36, 37].

4. Concluding remarks

Sampling of dust particles from the upper divertor region, i.e. the most critical area from the deposition point of view,

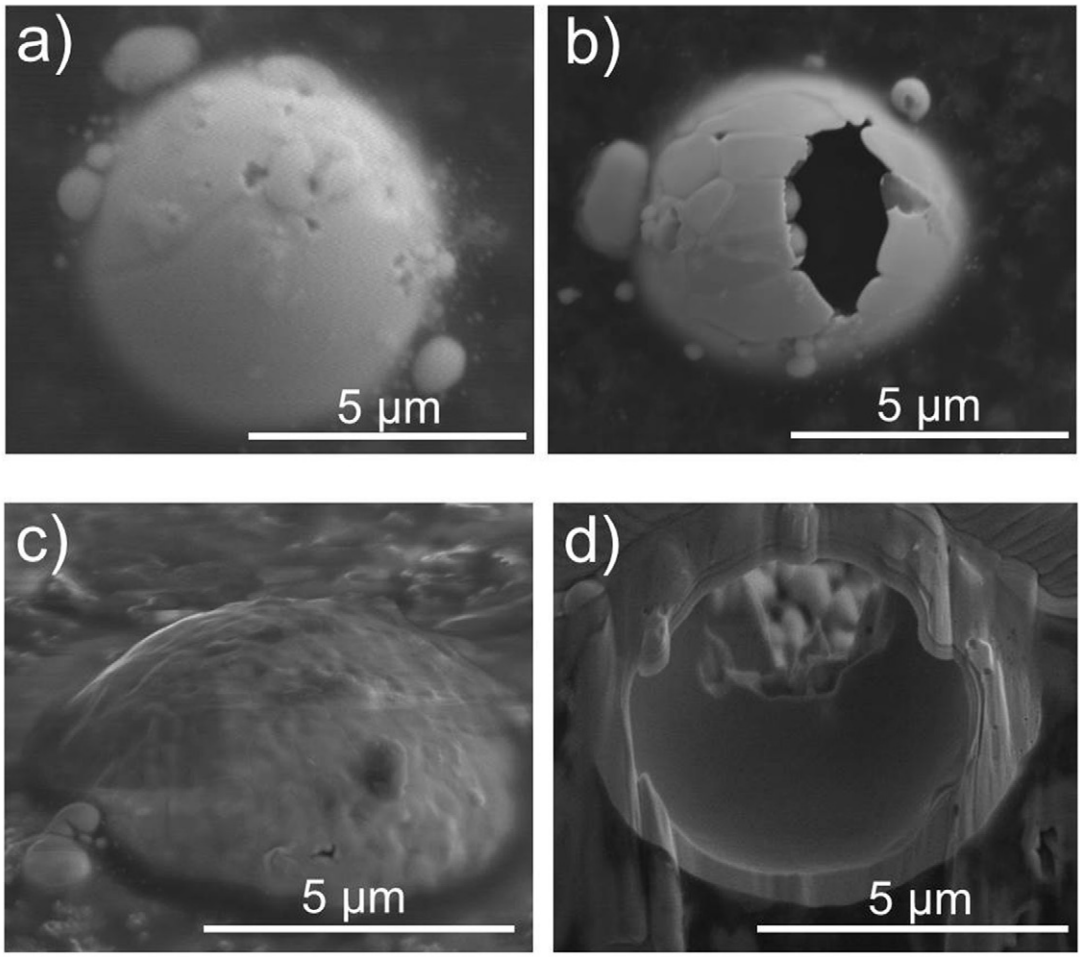

Figure 7. Tungsten rounded particles with recrystallized surfaces: topography of the closed shell (a) and the broken shell revealing the empty interior (b); particle selected for cross-sectional FIB/STEM studies (c) and the FIB-made cross-section proving the ball-like or bubble structure of the particle (d).

has allowed for a broad survey of particles, despite problems related to collection and handling of Be- and T-contaminated matter. These are the first results from a machine with PFC made of beryllium and tungsten. The most important contribution of this work to the knowledge of dust generation in fusion devices is the evidence proving the formation of two types of beryllium particles: flakes of co-deposits and small droplets. Both types of beryllium-rich particles are of great importance for ITER [38].

In the case of tungsten-based particles also two main forms were found: agglomerates originating from the coatings and spheroids. From the ITER point of view agglomerates are of secondary importance as no coated PFCs are planned. It is the formation of droplets, splashes and empty spheroids or bubbles which is a concern. The empty spheroids have been found in ASDEX Upgrade [11] and in JET-ILW, i.e. two machines using W coatings. Therefore, it is not possible to judge whether the formation of such objects is a general feature of tungsten or it is specific for coatings which—under erosion conditions—may detach as small flakes clustering together in the SOL. The issue is quite important because the assessment of the mass loss by dust generation fundamentally depends on the material density. Taking into account a sphere of 5 μm in diameter, such as shown in figures 7(c) and (d), one would estimate its mass as 1.25×10^{-9} g for a solid droplet or a factor of two less, 0.6×10^{-9} g, for a sphere/bubble with a 0.5 μm thick shell. It should also be added here that no comet-like metal splashes, often seen in TEXTOR [9], have been identified in the material under examination. Further studies are foreseen if there are droplets formed/deposited on the solid tungsten lamellae on Tile 5.

In summary, the identification and size determination of various Be and W particles will also be useful for the development and benchmarking of codes simulating dust formation and transport [39]. Taking into account the material handling issues (contamination) and resources (time/manpower) needed for a single particle examination by SEM/FIB/TEM a study of size distribution may become possible as a part of a long and broad statistical analysis. It should also be stressed again that the total amount of dust collected by vacuuming in JET-ILW was very small. It is also positive information that only a tiny number of flakes could be detached by the sticker, thus confirming the overall small amount of loose matter and a good adherence of Be-rich deposits to the divertor tile surface. Further detailed dust surveys from selected sets of tiles from the divertor and

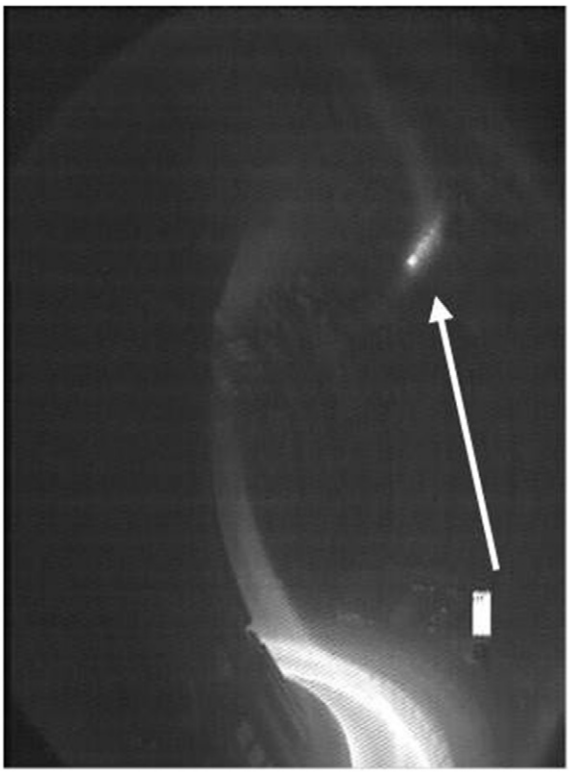

Figure 8. Operation of the reciprocating probe (located at the top of the JET vacuum vessel) made of boron nitride associated with outgassing and the release of BN particles.

JET main chamber has been planned, and dust collection on sticky pads has been done as a part of scientific activity during JET shut-down in 2015.

Acknowledgments

This work has been carried out within the framework of the EUROfusion Consortium and has received funding from the Euratom research and training programme 2014–2018 under grant agreement No 633053. The views and opinions expressed herein do not necessarily reflect those of the European Commission. The work has been partly funded by the Swedish Research Council (VR) through contract no. 621-2012-4148.

References

[1] Winter J. 1998 *Plasma Phys. Control. Fusion* **40** 1201
[2] Winter J. and Gebauer G. 1999 *J. Nucl. Mater.* **266–269** 228
[3] Rubel M. *et al* 2001 *Nucl. Fusion* **41** 1087
[4] Linke J. *et al* 2001 *Phys. Scr.* **T91** 36
[6] Fortuna E. *et al* 2007 *J. Nucl. Mater.* **367–370** 1507
[7] Ivanova D. *et al* 2009 *Phys. Scr*. **T138** 014012
[8] Ivanova D. *et al* 2011 *J. Nucl. Mater.* **415** S801
[9] Fortuna E. *et al* 2015 *Phys. Scr.* in press
[10] Rohde V. *et al* 2009 *Phys. Scr.* **T138** 014024
[11] Fortuna E. *et al* 2014 *Phys. Scr.* **T159** 014066
[12] Balden M. *et al* 2014 *Nucl. Fusion* **54** 073010
[13] Balden M. *et al* 2015 Comparison of chemical composition and morphology of dust particles from various fusion devices *Proc. PFMC-15, A-016/P-12 (Aix-en-Provence, France)*
[14] Coad J. P. *et al* 2001 *J. Nucl. Mater.* **290–293** 224
[15] Likonen J. *et al* 2013 *J. Nucl. Mater.* **438** S139
[16] Widdowson A. *et al* 2014 *Phys. Scr.* **T159** 014010
[17] Pegourie B. *et al* 2013 *J. Nucl. Mater.* **438** S120
[18] Rudakov D. L. *et al* 2009 *Nucl. Fusion* **49** 085022
[19] Hong S.-H. *et al* 2013 *Nucl. Instrum. Methods* **A720** 105
[20] Braams B. 2011 Characterisation of size, composition and origins of dust in fusion devices (www-nds.iaea.org/reports-new/indc-reports)
[21] Matthews G. F. *et al* 2009 *Phys. Scr.* **T138** 014030
[22] Matthews G. F. *et al* 2011 *Phys. Scr.* **T145** 014001
[23] Matthews G. F. *et al* 2013 *J. Nucl. Mater.* **438** S2
[24] Brezinsek S. *et al* 2015 *J. Nucl. Mater.* **463** 1
[25] Stork D. (ed) 1999 Technical aspects of deuterium–tritium operation at JET *Fusion Eng. Des.* **47** 205–31
[26] Widdowson A. *et al* 2013 *J. Nucl. Mater.* **438** S827
[27] Rubel M. *et al* 2013 *J. Nucl. Mater.* **438** S1204
[28] Coad J. P. *et al* 2014 *Phys. Scr.* **T159** 014009
[29] Likonen J. *et al* 2014 *Phys. Scr.* **T159** 014016
[30] Petersson P. *et al* 2015 *J. Nucl. Mater.* **463** 814
[31] Mayer M. *et al* 2015 Erosion and deposition in the JET divertor during the first ILW campaign *Proc. PFMC-15* (*Aix-en-Provence, France*, *1–13 May 2015*)
[32] Baron-Wiechec A. *et al* 2015 *J. Nucl. Mater.* **463** S157
[33] Johnson W. L. 1999 *MRS Bull.* **24** 42
[34] Bykov V. *et al* 2015 *Nucl. Instrum. Methods* **342** 19
[35] Fortuna E. *et al* 2007 *Phys. Scr.* **T128** 162
[36] Rubel M. *et al* 2001 *Eur. Conf. Abstr.* **25A** 1609
[37] Rubel M., Coad J. P. and Hole D. 2005 *Vacuum* **78** 255
[38] De Temmerman G. *et al* 2015 Dust in ITER: creation rates, diagnosis and analysis *Proc. PFMC-15* (*Aix-en-Provence, France*, *1–13 May 2015*)
[39] Ratynskaia S. *et al* 2013 *Nucl. Fusion* **53** 123002
[40] Romanelli F. *et al* 2015 *Nucl. Fusion* **55** 104001